MATERIALS CHEMISTRY
FRONTIERS

RESEARCH ARTICLE

View Article Online
View Journal | View Issue

Cite this: *Mater. Chem. Front.*, 2019, **3**, 2066

Tunable aggregation-induced circularly polarized luminescence of chiral AIEgens *via* the regulation of mono-/di-substituents of molecules or nanostructures of self-assemblies†

Shuwei Zhang, *[a] Jie Fan,[a] Yuxiang Wang,[b] Dong Li,[a] Xiaodong Jia,[a] Yu Yuan[a] and Yixiang Cheng *[b]

Received 31st May 2019,
Accepted 24th July 2019

DOI: 10.1039/c9qm00358d

rsc.li/frontiers-materials

Four chiral AIE-active luminogens (AIEgens) containing tetraphenylethene (TPE) and one or two chiral glutamic moieties connected by thiourea were designed and synthesized. All AIEgens showed tunable aggregation-induced circularly polarized luminescence (AICPL) by adjusting the mono-/di-substituents of molecules or nanostructures of self-assemblies. The enantiotopic mono-substituted compounds (**TPE-Glu**) exhibited mirror-imaged AICPL signals with the maximal $|g_{lum}|$ value of up to 0.02. Interestingly, the di-substituted *cis*- and *trans*-isomers showed reverse AICPL signals compared with those of mono-substituted ones. *cis*- and *trans*-isomers (**TPE-DGlu**) showed similar AICPL properties, whose signs of AICPL signals reversed while the water fraction (f_w) was more than 80%. The SEM images of their self-assemblies indicated that the AICPL properties should have an intrinsic relation with their molecular structures or self-assembled nanostructures.

Introduction

Circularly polarized luminescence (CPL) refers to the phenomenon that chiral luminescent substances emit different ratios of left and right circularly polarized light, which has been attracting increasing attention due to its special properties and potential applications in various fields such as the investigation of the excited chiral molecular structures, 3D optical displays, information storage and processing, molecular switches, biological detection and probing.[1] Up to now, different CPL systems have been reported, such as chiral organic conjugated molecules, polymers, organogels, and lanthanide complexes.[2] However, most conventional organic conjugated materials suffer from aggregation-caused quenching (ACQ) effect in the solid state, which greatly limits their applications in optics.[3] In 2001, Tang *et al.* first proposed aggregation-induced emission (AIE), which is used to describe the phenomenon that substances exhibit non-emissive behavior in a solution but have strong emission in the aggregated state.[4] Therefore, the AIE property provides an approach to prepare CPL materials with high emission intensity in the solid state. Tang *et al.* originally combined AIE and CPL and prepared a compound by introducing chiral D-mannose moiety into an AIE-active silole in 2012, which exhibited no CPL signal in solution but high AICPL signal in the aggregated state.[5] Since then, some other AIE-active CPL materials have been reported in different research fields.[6] Among them, supramolecular assemblies formed through non-covalent interactions have received considerable attention because the chiral assemblies usually possess better CPL properties than those of chiral molecules and could transfer CPL-silence molecular chirality to CPL-on chiral nanostructures.[7]

It is well-known that molecular chirality has great influence on the optical activity of chiral compounds.[8] However, the impact of *cis*- and *trans*-isomers on the optical activity of chiral molecules, particularly for the CPL property has rarely been studied.[9] Although several studies have reported the influence of nanostructures on the AICPL property, it is still valuable to design chiral supramolecular systems that could be effectively regulated to obtain chiral materials with a tunable AICPL property.[10]

Herein, we designed and synthesized four compounds, which contained AIE-active tetraphenylethene (TPE) and one or two chiral glutamic moieties connected by thiourea. The enantiotopic mono-substituent compounds are labelled as **TPE-L-Glu** and **TPE-D-Glu**, while the di-substituent *cis*- and *trans*-isomers are marked as *cis*-**TPE-L-DGlu** and *trans*-**TPE-L-DGlu**, respectively. Both mono- and di-substituted compounds exhibited

[a] *School of Chemistry and Chemical Engineering, Yangzhou University, Yangzhou, 225002, P. R. China. E-mail: shuweiz@yzu.edu.cn*
[b] *Key Lab of Mesoscopic Chemistry of MOE and Collaborative Innovation Center of Chemistry for Life Sciences, School of Chemistry and Chemical Engineering, Nanjing University, Nanjing 210023, P. R. China. E-mail: yxcheng@nju.edu.cn*

† Electronic supplementary information (ESI) available. See DOI: 10.1039/c9qm00358d

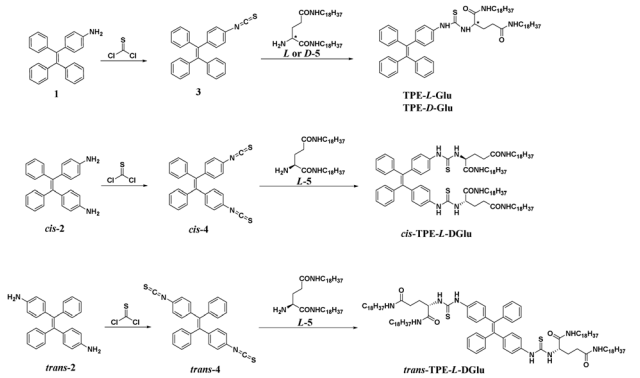

Scheme 1 Synthetic procedures for the preparation of **TPE-L-Glu**, **TPE-D-Glu**, *cis*-**TPE-L-DGlu** and *trans*-**TPE-L-DGlu**.

very weak emission and optical activity in THF, but showed obviously increasing fluorescence and tunable aggregation-induced circular dichroism (CD) and circularly polarized luminescence (CPL) signals with the addition of water, which demonstrated typical AIE and AICPL properties. The enantiotopic mono-substituted compounds (**TPE-Glu**) exhibited mirror-imaged AICPL signals, and the $|g_{lum}|$ value could reach 0.02 when water fraction (f_w) was at 50%. However, the di-substituted *cis*- and *trans*-isomers showed reverse AICPL signals compared with mono-substituted ones even when the same chiral glutamic moiety was used. *cis*-**TPE-L-DGlu** and *trans*-**TPE-L-DGlu** displayed similar optically active properties, whose aggregation-induced CD and CPL signals in more than 80% f_w mixed solvents was very different from those in less than 80% f_w mixed solvents. The SEM images of their self-assemblies indicated that AICPL properties could be related to both molecular structures and microstructures of the formed nanostructures (Scheme 1).

Experimental

Preparation of compound 3

A mixture of compound **1** (0.50 g, 1.44 mmol) and triethylamine (0.6 mL, 4.32 mmol) was dissolved in 15 mL dichloromethane, followed by the addition of thiophosgene (0.15 mL, 1.96 mmol) in an ice bath. The reaction mixture was stirred for 4 h at ambient temperature. Then, 30 mL dichloromethane was added, and the mixture was washed with water and saturated brine, and then dried over anhydrous Na_2SO_4. After the solvent was removed under reduced pressure to obtain the residue, which was purified by silica gel column chromatography (hexane/ethyl acetate, 20/1, v/v) compound **3** was obtained as a yellow oil (0.49 g, 87%). ^{1}H NMR (400 MHz, $CDCl_3$) δ (ppm): 6.95 (d, J = 7.1 Hz, 2H), 7.00 (d, J = 4.2 Hz, 7H), 7.13–7.10 (m, 10H). HRMS (ESI$^+$): m/z calcd [M$^+$] 389.1238; found 389.1316.

Preparation of *cis*-4 and *trans*-4

The same procedure as that of compound **3** was followed for *cis*-**4** and *trans*-**4**. The characterization of *cis*-**4**: ^{1}H NMR (400 MHz, $CDCl_3$) δ (ppm): 6.93 (d, J = 8.7 Hz, 6H), 6.96 (d, J = 9.4 Hz, 8H), 7.14 (s, 4H). HRMS (MALDI-TOF): m/z calcd [M$^+$] 446.0911; found 446.0945. The characterization of *trans*-**4**: ^{1}H NMR (400 MHz, $CDCl_3$) δ (ppm): 6.95 (d, J = 7.1 Hz, 2H), 7.00 (d, J = 4.2 Hz, 6H), 7.11 (dd, J = 8.2, 2.5 Hz, 10H). HRMS (MALDI-TOF): m/z calcd [M$^+$] 446.0911; found 446.0952.

Preparation of TPE-L-Glu and TPE-D-Glu

A mixture of compound **3** (0.50 g, 1.28 mmol) and compound L-**5** (1.67 g, 2.57 mmol) was dissolved in 30 mL of anhydrous THF. The reaction mixture was stirred for 4 h at 80 °C. After cooling to room temperature, the reaction mixture was concentrated to afford the residue, which was purified *via* silica gel column chromatography (CH_2Cl_2/MeOH, 20/1, v/v) to afford **TPE-L-Glu** as a pale-white powder (1.05 g, 77%). ^{1}H NMR (400 MHz, $CDCl_3$) δ (ppm): 0.86 (t, J = 6.6 Hz, 6H), 1.24 (s, 60H), 1.48–1.49 (m, 4H), 3.17–3.26 (m, 7H), 6.98–7.09 (m, 19H). HRMS (MALDI-TOF): m/z calcd [M + Na$^+$] 1061.7621; found 1061.7787. The prepared procedure of **TPE-D-Glu** was same as that for **TPE-L-Glu**. ^{1}H NMR (400 MHz, $CDCl_3$) δ (ppm): 0.81 (t, J = 6.0 Hz, 6H), 1.18 (s, 60H), 1.44 (d, J = 5.9 Hz, 4H), 3.12–3.19 (m, 5H), 4.86 (s, 1H), 5.75 (s, 1H), 6.90–7.04 (m, 19H). HRMS (MALDI-TOF): m/z calcd [M + Na$^+$] 1061.7621; found 1061.7802.

Preparation of *cis*-TPE-L-DGlu and *trans*-TPE-L-DGlu

The same procedure as that of **TPE-L-Glu** was used for *cis*-**TPE-L-DGlu** and *trans*-**TPE-L-DGlu**. The characterization of *cis*-**TPE-L-DGlu**: ^{1}H NMR (400 MHz, $CDCl_3$) δ (ppm): 0.86 (t, J = 6.2 Hz, 12H), 1.23 (s, 120H), 1.35(t, J = 7.3 Hz, 8H), 1.42 (s, 8H), 3.08–3.21 (m, 12H), 6.82 (d, J = 8.5 Hz, 4H), 6.97 (d, J = 3.7 Hz, 4H), 7.00–7.05 (m, 10H). HRMS (MALDI-TOF): m/z calcd [M + Na$^+$] 1768.3780; found 1768.3894. *trans*-**TPE-L-DGlu**: ^{1}H NMR (400 MHz, $CDCl_3$) δ (ppm): 0.86 (t, J = 6.6 Hz, 12H), 1.24 (s, 120H), 1.37–1.45 (m, 16H), 1.68 (d, J = 10.3 Hz, 4H), 3.11–3.17 (m, 4H), 6.86 (d, J = 8.3 Hz, 4H), 6.98 (d, J = 3.6 Hz, 4H), 7.01–7.10 (m, 10H). HRMS (MALDI-TOF): m/z calcd [M + Na$^+$] 1768.3780; found 1768.3960.

Preparation of samples for optical measurements

Several stock solutions of the compounds were first prepared in THF (0.20 mM). Then, 10 μL of the stock solution was transferred to 2 mL THF/water mixture to afford the test solutions at the concentration of 10 μM. The optical measurements were then performed after 2 h.

Preparation of samples for SEM

Different THF/water mixtures of **TPE-L-Glu**, **TPE-D-Glu**, *cis*-**TPE-L-DGlu** and *trans*-**TPE-L-DGlu** with concentrations of 10 μM were prepared. Then, 10 μL of the solutions was dropped onto the surface of Si wafers, which were dried in vacuum after 2 h. The as-prepared samples were characterized by SEM.

Results and discussions

Synthesis of chiral AIEgens

Compounds **1**, *cis*- and *trans*-**2**, L- and D-**5** were prepared according to previously reported procedures.[11] The initial compounds first

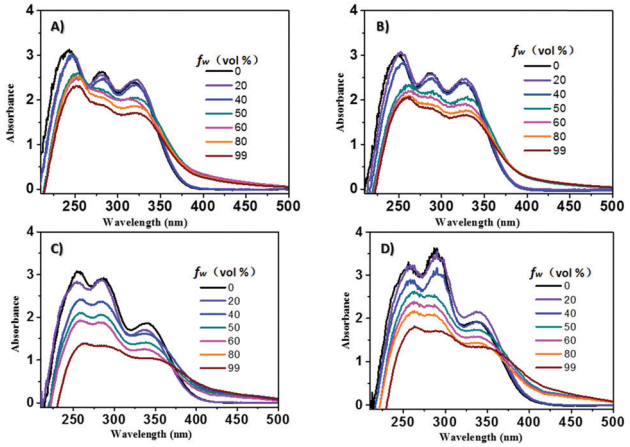

Fig. 1 UV-vis absorption spectra of (A) **TPE-L-Glu**, (B) **TPE-D-Glu**, (C) *cis*-**TPE-L-DGlu** and (D) *trans*-**TPE-L-DGlu** in THF/water mixture with different f_w. Concentration: 1×10^{-5} M.

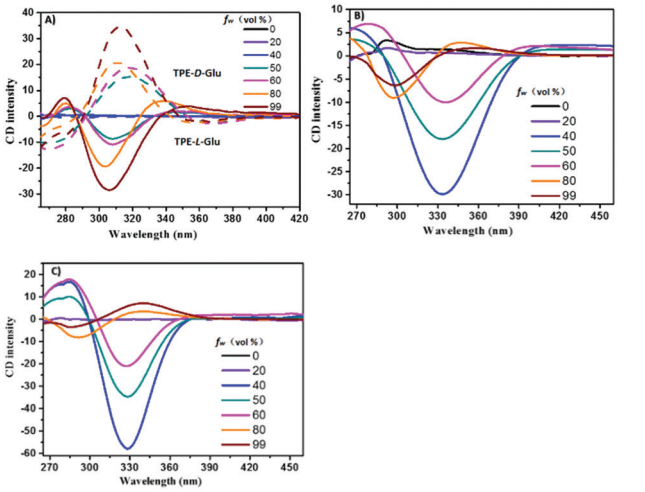

Fig. 2 CD spectra of (A) **TPE-D-Glu** and **TPE-L-Glu**, (B) *cis*-**TPE-L-DGlu**, (C) *trans*-**TPE-L-DGlu** in THF/water mixtures with different f_w. Solution concentration = 1×10^{-5} M.

reacted with thiophosgene to obtain mono- or di-isothiocyanato compounds **3** and *cis*- and *trans*-**4**. These intermediates then reacted with chiral glutamic derivatives (compound L- or D-**5**) to afford the four desired compounds. All the compounds were confirmed by NMR and HRMS (see ESI†).

Optical properties

The UV-vis spectra of these compounds were first obtained in a THF/water mixture, in which THF acted as a good solvent and water acted as a poor solvent. As shown in Fig. 1, the four compounds, **TPE-L-Glu**, **TPE-D-Glu**, *cis*-**TPE-L-DGlu** and *trans*-**TPE-L-DGlu**, exhibited similar absorption spectra with three absorption peaks located at about 250, 285 and 340 nm, respectively, which could result from the π–π* conjugation of the TPE cores. When f_w was increased in the mixture, the decreased absorbance and spectral tails in the long wavelength region were clear probably due to the formation of aggregates,[12] and the observed red-shift indicated that J-aggregate could be formed in the mixture.[13] Interestingly, the absorption spectra of **TPE-D-Glu** displayed a small red-shift of 7 nm compared to **TPE-L-Glu**, which might be ascribed to the different sizes of the formed nanoparticles.

Next, we investigated their CD spectra. As shown in Fig. 2A, the CD data of the mono-substituted compounds demonstrated that both compounds were CD silent in THF. However, the aggregation-induced CD (AICD) signals could be observed with an increase in f_w of the mixed solvents. The two enantiomers exhibited slightly deflected mirror-imaged AICD signals, whose signals were consistent with their absorption data. Moreover, we found that the AICD signals apparently enhanced with higher f_w, and could reach the maximum when f_w was at 99%.

As depicted in Fig. 2B and C, *cis*-**TPE-L-DGlu** presented a very weak signal at 290 nm in THF, while *trans*-**TPE-L-DGlu** had almost no signal at the same condition. The different AICD signals in THF between two isomers could result from the formation of the intramolecular hydrogen bond of the *cis*-isomer. Moreover, obvious aggregation-induced Cotton effects were observed with increased f_w. The negative signals at 330 nm of the isomers were highest when f_w was at 40%, *i.e.*, the CD signal of *trans*-isomer was about twice than that of *cis*-isomer probably due to the different hydrogen bonds of the inter- and intra-forms. However, the negative signals decreased and displayed a slight red-shift when water was present in the mixture until f_w was up to 60%. Furthermore, the negative signals at about 296 nm and positive signals at about 350 nm of *cis*-**TPE-L-DGlu** were detected when more water was added. The *trans*-isomer had similar negative and positive signals, which were related to those of the *cis*-isomer. All the above data indicated that the point chirality of the glutamic moiety could transfer to the TPE part in aggregates.

For the two di-substituted isomers, *trans–cis* isomerization could theoretically occur in the excited state. However, when the size of substituents or the interactions between the substituents increase, the *trans–cis* isomerization becomes much more difficult, according to the previous reported works.[11b,14] The fluorescence spectra of mono- and di-substituted compounds are shown in Fig. 3. As predicted, the four TPE-containing

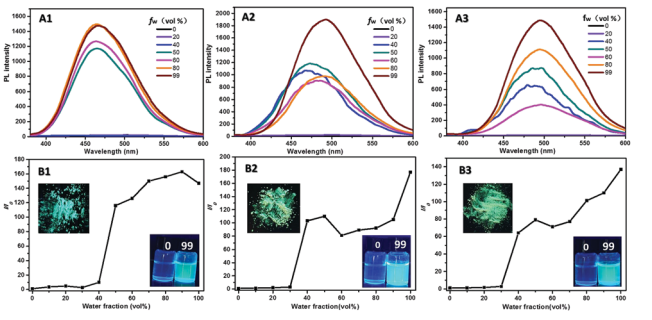

Fig. 3 Fluorescent spectra of **TPE-L-Glu**, *cis*-**TPE-L-DGlu** and *trans*-**TPE-L-DGlu** in THF/water mixed solvents with different f_w (A1–A3); plot of I/I_0 values *versus* f_w (B1–B3), where I_0 represents the emission intensity in THF. Concentration: 1×10^{-5} M; excitation wavelength: 340 nm. Inset: Photographs of **TPE-L-Glu**, *cis*-**TPE-L-DGlu** and *trans*-**TPE-L-DGlu** in solid and THF/water mixtures with 0 and 99% f_w under 365 nm UV lamp.

compounds were AIE-active. Their fluorescence intensities were relatively weak when f_w was less than 40% in the mixed solvents and enhanced rapidly with the addition of more water due to the formation of aggregates. The highest fluorescent intensities could increase to 164, 176 and 138 times for **TPE-L-Glu**, *cis*-**TPE-L-DGlu** and *trans*-**TPE-L-DGlu**, respectively. Both the aggregates in 99% f_w mixtures and their solids displayed high green emission. Moreover, the emission peaks shifted to longer wavelengths with increase in f_w, which further indicated the formation of J aggregates.

The aggregates exhibited strong fluorescence and obvious AICD signals, which inspired us to further investigate their CPL properties. As shown in Fig. 4A, **TPE-L-Glu** and **TPE-D-Glu** exhibited mirrored AICPL spectra in the region from 400 to 600 nm when f_w was higher than 50%. The highest AICPL signals decreased and red-shifted when more water was added to the mixed solvents. The CPL dissymmetry factor, g_{lum}, could reach 0.021 and −0.019 for **TPE-L-Glu** and **TPE-D-Glu**, respectively. Interestingly, the original AICPL signals of *cis*-**TPE-L-DGlu** and *trans*-**TPE-L-DGlu** exhibited opposite signs compared with **TPE-L-Glu** although they had the same chiral L-glutamic moiety, which could be attributed to the different intermolecular noncovalent interactions.[6a,15] The two di-substituted compounds possessed similar AICPL spectra with the highest signal at 60% f_w, and their AICPL signals could reverse when f_w was higher than 80%, whose g_{lum} values changed from −0.007 to 0.003 for *cis*-isomer, and from −0.008 to 0.002 for the *trans*-isomer, respectively. All the data indicated that the AICPL properties of these TPE derivatives could be adjusted by both the chirality of chiral source (L or D-stereoisomers) and the number of introduced substituents (mono- or di-substituted). The strength of the CPL signals could be tuned by changing f_w in the mixed solvents.

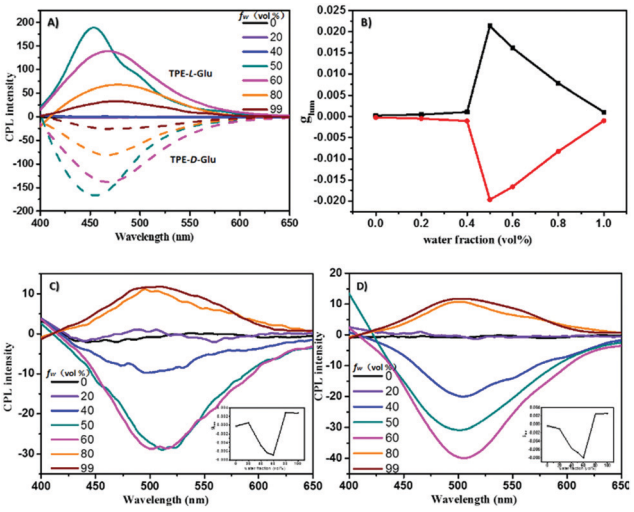

Fig. 4 CPL spectra of (A) **TPE-L-Glu** and **TPE-D-Glu**, (C) *cis*-**TPE-L-DGlu**, (D) *trans*-**TPE-L-DGlu** in THF/water mixed solvents. Concentration: 1×10^{-5} M; excitation wavelength: 340 nm. (B) g_{lum} *versus* f_w of **TPE-L-Glu** and **TPE-D-Glu**. Inset: g_{lum} *versus* f_w of *cis*-**TPE-L-DGlu** and *trans*-**TPE-L-DGlu**.

The morphologies of the aggregates

According to the above optical data, all the compounds displayed tunable aggregation-induced optically active properties by changing f_w of the mixed solvents, which stimulated us to investigate the relation between optical activities and supramolecular morphologies of the self-assembled aggregates. Moreover, to demonstrate the intermolecular interactions of the compounds even in THF, we obtained the SEM images of formed nanostructures after THF was volatilized. As shown in Fig. 5, the morphologies of formed self-assemblies were obviously different when the f_w of the mixed solvents was changed. For the enantiotopic mono-substituted compounds, the SEM images of the compounds in THF (10 μM) showed the formation of similar nanofibers, which further showed intermolecular interactions even in the molecular state. Thicker nanofibers were detected when f_w was increased to 40% due to the formation of aggregates. Moreover, helical nanofibers formed when 50% f_w was in the mixed solvents, which L-enantiomer produced left-handed twist nanofibers and D-enantiomer gave the right-handed ones. However, irregular nanoparticles formed after more water was added. The different morphologies of formed nanostructures could lead to the changes in the AICPL intensities. For *cis*- and *trans*-isomeric compounds, different irregular nanoparticles were detected in the mixed solvents probably due to the different intra- or intermolecular interactions. *cis*-**TPE-L-DGlu** with two L-glutamic moieties located at the same side experience intramolecular interactions that could lead to form nanoparticles to reduce energy.[16] However, *trans*-**TPE-L-DGlu** with two substituents on the opposite sides could undergo intermolecular weak interactions and self-assembled in side-by-side formation to generate nanoribbons.[17] The different noncovalent interactions resulted in the formation of diverse nanostructures and further affected the intensities of the AICPL signals of the two isomers. Note that the *trans*-one gave higher signals compared to the *cis*-one.

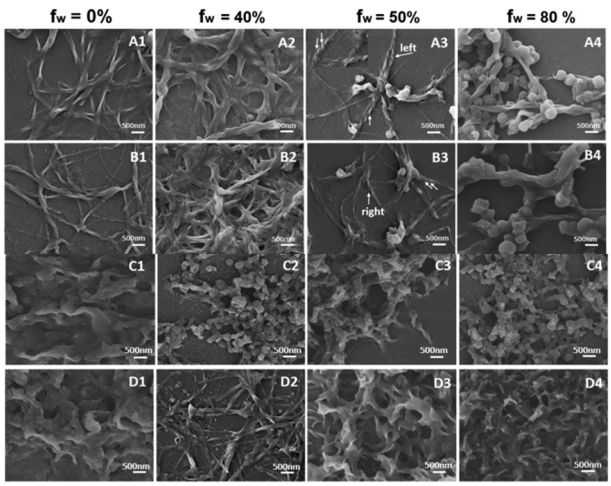

Fig. 5 SEM images of **TPE-L-Glu** (A1–A4), **TPE-D-Glu** (B1–B4), *cis*-**TPE-L-DGlu** (C1–C4), *trans*-**TPE-L-DGlu** (D1–D4) obtained from THF/water mixed solvents at different f_w. (A1–D1) 10/0; (A2–D2) 6/4; (A3–D3) 5/5; (A4–D4) 1/9. Concentration: 1×10^{-5} M.

The SEM images of the self-assemblies indicate that AICPL signals could be affected by the morphologies of formed microstructures, which the distinguishing formed nanostructures should originally ascribe to the different intermolecular interactions between the mono- and di-substituted AIEgens.

Conclusions

In conclusion, we designed and synthesized four chiral AIEgens containing TPE and one or two chiral glutamic moieties that were connected by thiourea. All the compounds exhibited aggregation-induced optical activities in a THF/water mixture. The enantiotopic mono-substituted compounds gave mirror-imaged AICPL signals, whose $|g_{lum}|$ value could reach 0.02. The di-substituted isomers showed opposed original AICPL signals compared with mono-substituted isomers although they had the same chiral glutamic moiety. *cis*- and *trans*-isomers displayed similar AICPL properties, whose signs of AICPL signals reversed when f_w was more than 80%. The SEM images of the self-assemblies indicated that AICPL properties could be related to the number of substituents in molecules and the formed self-assembled microstructures.

Conflicts of interest

There are no conflicts to declare.

Acknowledgements

We gratefully acknowledge for financial support from the National Natural Science Foundation of China (No. 21702180), Jiangsu Provincial Nature Science Foundation (SBK2016021885), the Top-notch Academic Programs Project of Jiangsu Higher Education Institutions, and the Priority Academic Program Development of Jiangsu Higher Education Institutions.

Notes and references

1 (*a*) Y. Ying, R. C. da Costa, D.-M. Smilgies, A. J. Campbell and M. J. Fuchter, *Adv. Mater.*, 2013, **25**, 2624; (*b*) M. Li, S.-H. Li, D. Zhang, M. Cai, L. Duan, M.-K. Fung and C.-F. Chen, *Angew. Chem., Int. Ed.*, 2018, **57**, 2889; (*c*) J. R. Brandt, X. Wang, Y. Yang, A. J. Campbell and M. J. Fuchter, *J. Am. Chem. Soc.*, 2016, **138**, 9743; (*d*) W. Li, Z. J. Coppens, L. V. Besteiro, W. Wang, A. O. Govorov and J. Valentine, *Nat. Commun.*, 2015, **6**, 8379; (*e*) J. Kumar, T. Nakashima, H. Tsumatori and T. Kawai, *J. Phys. Chem. Lett.*, 2014, **5**, 316; (*f*) H. Ruthanne, E. J. Swain, N. I. Hammer, D. Venkataraman and M. D. Barnes, *Science*, 2006, **314**, 1437; (*g*) C. Chen, J. Chen, T. Wang and M. Liu, *ACS Appl. Mater. Interfaces*, 2016, **8**, 30608; (*h*) M. Shimada, Y. Yamanoi, T. Ohto, S.-T. Pham, R. Yamada, H. Tada, K. Omoto, S. Tashiro, M. Shionoya, M. Hattori, K. Jimura, S. Hayashi, H. Koike, M. Iwamura, K. Nozaki and H. Nishihara, *J. Am. Chem. Soc.*, 2017, **139**, 11214; (*i*) F. Song, Z. Xu, Q. Zhang, Z. Zhao, H. Zhang, W. Zhao, Z. Qiu, C. Qi, H. Zhang, H. H. Y. Sung, I. D. Williams, J. W. Y. Lam, Z. Zhao, A. Qin, D. Ma and B. Z. Tang, *Adv. Funct. Mater.*, 2018, **28**, 1800051.

2 (*a*) K. Nakamura, S. Furumi, M. Takeuchi, T. Shibuya and K. Tanaka, *J. Am. Chem. Soc.*, 2014, **136**, 5555; (*b*) T. Wu and P. Bouř, *Chem. Commun.*, 2018, **54**, 1790; (*c*) Y. Wang, X. Li, L. Yang, W. Y. Sun, C. Zhu and Y. Cheng, *Mater. Chem. Front.*, 2018, **2**, 554; (*d*) Y. Nagata, M. Uno and M. Suginome, *Angew. Chem., Int. Ed.*, 2016, **55**, 7126; (*e*) J. Zhang, Q. Liu, W. Wu, J. Peng, H. Zhang, F. Song, B. He, X. Wang, H. H.-Y. Sung, M. Chen, B. S. Li, S. H. Liu, J. W. Y. Lam and B. Z. Tang, *ACS Nano*, 2019, **13**, 3618; (*f*) B. Zhao, K. Pan and J. Deng, *Macromolecules*, 2018, **51**, 7104; (*g*) Y. Chen, X. Li, N. Li, Y. Quan, Y. Cheng and Y. Tang, *Mater. Chem. Front.*, 2019, **3**, 867; (*h*) N. Zhao, W. Gao, M. Zhang, J. Yang, X. Zheng, Y. Li, R. Cui, W. Yin and N. Li, *Mater. Chem. Front.*, 2019, **3**, 1613.

3 (*a*) W. Z. Yuan, P. Lu, S. Chen, J. W. Y. Lam, Z. Wang, Y. Liu, H. S. Kwok, Y. Ma and B. Z. Tang, *Adv. Mater.*, 2010, **22**, 2159; (*b*) S. W. Thomas, G. D. Joly and T. M. Swager, *Chem. Rev.*, 2007, **107**, 1339; (*c*) J. Liang, B. Z. Tang and B. Liu, *Chem. Soc. Rev.*, 2015, **44**, 2798; (*d*) A. S. Klymchenko, *Acc. Chem. Res.*, 2017, **50**, 366.

4 (*a*) J. D. Luo, Z. L. Xie and B. Z. Tang, *Chem. Commun.*, 2001, 1740; (*b*) J. Mei, N. L. C. Leung, R. T. K. Kwok, J. W. Y. Lam and B. Z. Tang, *Chem. Rev.*, 2015, **115**, 11718.

5 J. Liu, H. Su, L. Meng, Y. Zhao, C. Deng, J. C. Y. Ng, P. Lu, M. Faisal, J. W. Y. Lam, X. Huang, H. Wu, K. S. Wong and B. Z. Tang, *Chem. Sci.*, 2012, **3**, 2737.

6 (*a*) H. Li, J. Cheng, Y. Zhao, J. W. Y. Lam, K. S. Wong, H. Wu, B. S. Li and B. Z. Tang, *Mater. Horiz.*, 2014, **1**, 518; (*b*) X. Liu, J. Jiao, X. Jiang, J. Li, Y. Cheng and C. Zhu, *J. Mater. Chem. C*, 2013, **1**, 4713; (*c*) S. Zhang, Y. Wang, F. Meng, C. Dai, Y. Cheng and C. Zhu, *Chem. Commun.*, 2015, **51**, 9014; (*d*) Q. Liu, Q. Xia, S. Wang, B. S. Li and B. Z. Tang, *J. Mater. Chem. C*, 2018, **6**, 4807; (*e*) J. Roose, B. Z. Tang and K. S. Wong, *Small*, 2016, **12**, 6495; (*f*) G. Huang, R. Wen, Z. Wang, B. S. Li and B. Z. Tang, *Mater. Chem. Front.*, 2018, **2**, 1884.

7 (*a*) E. M. Sánchez-Carnerero, A. R. Agarrabeitia, F. Moreno, B. L. Maroto, G. Muller, M. J. Ortiz and S. de la Moya, *Chem. – Eur. J.*, 2015, **21**, 13488; (*b*) Y. Zhang, D. Yang, J. Han, J. Zhou, Q. Jin, M. Liu and P. Duan, *Langmuir*, 2018, **34**, 5821; (*c*) T. Goto, Y. Okazaki, M. Ueki, Y. Kuwahara, M. Takafuji, R. Oda and H. Ihara, *Angew. Chem., Int. Ed.*, 2017, **56**, 2989; (*d*) E. Yashima, N. Ousaka, D. Taura, K. Shimomura, T. Ikai and K. Maeda, *Chem. Rev.*, 2016, **116**, 13752; (*e*) D. Niu, Y. Jiang, L. Ji, G. Ouyang and M. Liu, *Angew. Chem., Int. Ed.*, 2019, **58**, 5946.

8 (*a*) H. Rhee, I. Eom, S.-H. Ahn and M. Cho, *Chem. Soc. Rev.*, 2012, **41**, 4457; (*b*) F. S. Richardson, *Chem. Rev.*, 1979, **79**, 17.

9 (*a*) J. Wang, J. Mei, R. R. Hu, J. Z. Sun, A. J. Qin and B. Z. Tang, *J. Am. Chem. Soc.*, 2012, **134**, 9956; (*b*) C.-J. Zhang, G. Feng, S. Xu, Z. Zhu, X. Lu, J. Wu and B. Liu, *Angew. Chem., Int. Ed.*, 2016, **55**, 6192; (*c*) X. F. Fang, Y.-M. Zhang, K. Chang, Z. Liu, X. Su, H. Chen, S. X.-A. Zhang, Y. Liu and C. Wu, *Chem. Mater.*, 2016, **28**, 6628.

10 (*a*) Q. Ye, D. Zhu, H. Zhang, X. Lu and Q. Lu, *J. Mater. Chem. C*, 2015, **3**, 6997; (*b*) B. S. Li, R. Wen, S. Xue, L. Shi, Z. Tang, Z. Wang and B. Z. Tang, *Mater. Chem. Front.*, 2017, **1**, 646; (*c*) H. Li, B. S. Li and B. Z. Tang, *Chem. – Asian J.*, 2019, **14**, 674; (*d*) J. Han, J. You, X. Li, P. Duan and M. Liu, *Adv. Mater.*, 2017, **29**, 1606503; (*e*) S. Zhang, Y. Sheng, G. Wei, Y. Quan, Y. Cheng and C. Zhu, *Polym. Chem.*, 2015, **6**, 2416; (*f*) J. Li, C. Yang, C. Huang, Y. Wan and W.-Y. Lai, *Tetrahedron Lett.*, 2016, **57**, 1256.

11 (*a*) M. Luo, X. Zhou, Z. Chi, S. Liu, Y. Zhang and J. Xu, *Dyes Pigm.*, 2014, **101**, 74; (*b*) H.-Q. Peng, X. Zheng, T. Han, R. T. K. Kwok, J. W. Y. Lam, X. Huang and B. Z. Tang, *J. Am. Chem. Soc.*, 2017, **139**, 10150; (*c*) T. Matsumoto, F. Yamada and T. Kurosaki, *Macromolecules*, 1997, **12**, 3547; (*d*) Y. Li, T. Wang and M. Liu, *Soft Matter*, 2007, **3**, 1312.

12 (*a*) N. J. Hestand and F. C. Spano, *Acc. Chem. Res.*, 2017, **50**, 341; (*b*) C. Dai, D. Yang, W. Zhang, B. Bao, Y. Cheng and L. Wang, *Polym. Chem.*, 2015, **6**, 3962.

13 (*a*) M. E. Ziffer, S. B. Jo, Y. Liu, H. Zhong, J. C. Mohammed, J. S. Harrison, A. K.-Y. Jen and D. S. Ginger, *J. Phys. Chem. C*, 2018, **122**, 18860; (*b*) V. Grande, B. Soberats, S. Herbst, V. Stepanenko and F. Würthner, *Chem. Sci.*, 2018, **9**, 6904; (*c*) S. B. Anantharaman, T. Stöferle, F. A. Nüesch, R. F. Mahrt and J. Heier, *Adv. Funct. Mater.*, 2019, **29**, 1806997.

14 (*a*) J. Li, X. Peng, C. Huang, Q. Qi, W.-Y. Lai and W. Huang, *Polym. Chem.*, 2018, **9**, 5278; (*b*) J. Li, C. Yang, X. Peng, Y. Chen, Q. Qi, X. Luo, W.-Y. Lai and W. Huang, *J. Mater. Chem. C*, 2018, **6**, 19; (*c*) X. Fang, Y.-M. Zhang, K. Chang, Z. Liu, X. Su, H. Chen, S. X.-A. Zhang, Y. Liu and C. Wu, *Chem. Mater.*, 2016, **28**, 6628.

15 (*a*) H. Li, J. Cheng, H. Deng, E. Zhao, B. Shen, J. W. Y. Lam, K. S. Wong, H. Wu, B. S. Li and B. Z. Tang, *J. Mater. Chem. C*, 2015, **3**, 2399; (*b*) H. Li, X. Zheng, H. Su, J. W. Y. Lam, K. S. Wong, S. Xue, X. Huang, X. Huang, B. S. Li and B. Z. Tang, *Sci. Rep.*, 2016, **6**, 19277.

16 (*a*) I. H. Nayyar, E. R. Batista, S. Tretiak, A. Saxena, D. L. Smith and R. L. Martin, *J. Polym. Sci., Part B: Polym. Phys.*, 2013, **51**, 935; (*b*) A. Declemy, C. Rulliere and P. Kottis, *Chem. Phys. Lett.*, 2017, **101**, 401; (*c*) Y.-Z. Zheng, Y. Zhou, Q. Liang, D.-F. Chen, R. Guo, C.-L. Xiong, X.-J. Xu, Z.-N. Zhang and Z.-J. Huang, *Dyes Pigm.*, 2017, **141**, 179.

17 (*a*) H. Zhang, C. Guo, X. Wang, J. Xu, X. He, Y. Liu, X. Liu, H. Huang and J. Sun, *Cryst. Growth Des.*, 2013, **13**, 679; (*b*) Z. Wang, Y. Gong, L. Zhang, C. Jing, F. Gao, S. Zhang and H. Li, *Chem. Eng. J.*, 2018, **342**, 238; (*c*) C. Chen, T. Wang, Y. Fu and M. Liu, *Chem. Commun.*, 2016, **52**, 1381.